

Test of Chiral Perturbation Theory in kaon decays

C. Lazzeroni^{a*}

^aSchool of Physics and Astronomy, The University of Birmingham, Edgbaston, Birmingham, B15 2TT, United Kingdom

This paper presents results obtained by the CERN experiment NA48/2. Sample of 7146 $K^\pm \rightarrow \pi^\pm e^+ e^-$ decays, of 1164 $K^\pm \rightarrow \pi^\pm \gamma \gamma$ events and of 120 $K^\pm \rightarrow \pi^\pm \gamma e^+ e^-$ events have been collected with small background contamination. Branching ratio and form factors for three different models have been obtained for $K^\pm \rightarrow \pi^\pm e^+ e^-$, plus a model-independent branching ratio. In addition, the first measurement of the direct CP violating asymmetry has been performed. A measurement of the branching ratio has been obtained for $K^\pm \rightarrow \pi^\pm \gamma \gamma$, and kinematic distributions have been compared to ChPT expectations. Finally, the branching ratio of $K^\pm \rightarrow \pi^\pm \gamma e^+ e^-$ has been measured in the kinematically accessible region, representing the first observation of such a decay.

1. Introduction

Radiative non-leptonic kaon decays give information on the structure of the weak interactions at low energies, and provide crucial tests of Chiral Perturbation Theory (ChPT). This paper presents new results for $K^\pm \rightarrow \pi^\pm e^+ e^-$, $K^\pm \rightarrow \pi^\pm \gamma \gamma$ and $K^\pm \rightarrow \pi^\pm \gamma e^+ e^-$ decays obtained by the NA48/2 experiment at the CERN SPS.

The flavour-changing neutral current process $K^\pm \rightarrow \pi^\pm e^+ e^-$ is induced at one-loop level in the Standard Model and it is highly suppressed by the GIM mechanism. This decay has been described by the ChPT [1]. Several models predict the shape of the dilepton invariant mass spectrum, and the decay rate [2,3]. This decay was first studied at CERN[4], followed by the BNL/E777[5] and E865[6] measurements.

The $K^\pm \rightarrow \pi^\pm \gamma \gamma$ and $K^\pm \rightarrow \pi^\pm \gamma e^+ e^-$ decays similarly arise at one-loop level in ChPT. The decay rates and spectra have been computed at leading and next-to-leading orders[7,8], and strongly depend on a single theoretically unknown parameter c . Before the NA48/2 experiment, only a single observation of 31 $K^\pm \rightarrow \pi^\pm \gamma \gamma$ candidates was made[9], while the $K^\pm \rightarrow \pi^\pm \gamma e^+ e^-$ decay has never been observed.

The NA48/2 experiment[10] uses simultaneous K^+ and K^- beams produced by 400 GeV/c pri-

mary SPS protons impinging at zero incidence angle on a beryllium target. The kaon decay volume is housed in a 114 m long cylindrical vacuum tank. The decay volume is followed by a magnetic spectrometer located in a tank filled with helium at nearly atmospheric pressure, separated from the vacuum tank by a thin (0.31% X^0) Kevlar composite window. The magnet provides a horizontal transverse momentum kick of $p = 120$ MeV/c for charged particles. The magnetic spectrometer is followed by a plastic scintillator hodoscope used to produce fast trigger signals and to provide precise time measurements of charged particles. The hodoscope is followed by a liquid krypton electromagnetic calorimeter used for photon detection and particle identification. In order to simulate the detector response, a detailed GEANT-based[11] Monte Carlo simulation is used, which includes full detector geometry and material description, stray magnetic fields, spectrometer local inefficiencies and misalignment, detailed simulation of the kaon beam line, and time variations of the above throughout the running period. Radiative corrections are applied to kaon decays using the PHOTOS package[12].

2. $K^\pm \rightarrow \pi^\pm e^+ e^-$ decays

The decay is supposed to proceed through a Feynman diagram with one photon exchange, re-

*On behalf of the NA48 Collaboration.

sulting in a spectrum of the $z = (M_{ee}/M_K)^2$ kinematic variable sensitive to the form factor $W(z)$:

$$d\Gamma/dz = \frac{\alpha^2 M_K}{12\pi(4\pi)^4} \lambda^{3/2}(1, z, r_\pi^2) \times \sqrt{(1 - 4r_e^2/z)(1 + 2r_e^2/z)} |W(z)|^2 \quad (1)$$

where $r_e = M_e/M_K$, $r_\pi = M_\pi/M_K$, $\lambda(a, b, c) = a^2 + b^2 + c^2 - 2ab - 2ac - 2bc$.

The distribution of the angle $\theta_{\pi e}$ in the e^+e^- rest frame is proportional to $\sin^2\theta_{\pi e}$ and it is insensitive to $W(z)$. The following parameterizations of the form factor $W(z)$ are considered in the present analysis:

- Linear: $W(z) = G_F M_K^2 f_0 (1 + \delta z)$ with parameters f_0 and δ as normalization and slope
- Next-to-Leading order in ChiPT[2]: $W(z) = G_F M_K^2 (a_+ + b_+ z) W^{\pi\pi}(z)$ with free parameters a, b and a pion loop term
- ChiPT parameterization involving meson form factors[3]: $W(z) = W(M_a, M_b, z)$ with resonance masses M_a and M_b treated as free parameters

The goal of the analysis is the extraction of the form factor parameters in the framework of each of the above models, and to compute the corresponding branching fractions.

2.1. Selection

Three-track vertices (compatible with the topology of $K^\pm \rightarrow \pi^\pm e^+ e^-$ and $K^\pm \rightarrow \pi^\pm \pi_D^0$ decays) are reconstructed using the Kalman filter algorithm[13] by extrapolation of track segments from the upstream part of the spectrometer back into the decay volume. The measured Earth's magnetic field, the stray field due to magnetization of the vacuum tank, and the multiple scattering in the Kevlar window are taken into account. Tracks must satisfy quality criteria and particle identification is performed using the ratio E/p of track energy deposition in the calorimeter to its momentum measured by the spectrometer. Suppression of the $K^\pm \rightarrow \pi^\pm \pi_D^0$ background is achieved applying the criteria $z = (M_{ee}/M_K)^2 > 0.08$, which approximately corresponds to $M_{ee} > 140 \text{ MeV}/c^2$.

Both signal and normalization samples are recorded via the same two-level trigger chain. At the first level (L1), a coincidence of hits in the two planes of the HOD in at least two of the 16 non-overlapping segments is required. The second level (L2) is based on a hardware system computing coordinates of hits from spectrometer drift times, and a farm of asynchronous processors performing fast track reconstruction and running a selection algorithm. Such algorithm basically requires at least two tracks to originate in the decay volume with the closest distance of approach being less than 5 cm. L1 triggers not satisfying this condition are examined further and accepted, if there is a reconstructed track not kinematically compatible with a $\pi^\pm \pi^0$ decay of a K^\pm having momentum of 60 GeV/c directed along the beam axis. Direct measurements of trigger inefficiencies are not possible for $K^\pm \rightarrow \pi^\pm e^+ e^-$, due to very limited sizes of the corresponding control samples. Dedicated simulations of L1 and L2 performance were used instead. The simulated efficiencies and their kinematic dependencies were compared against measurements for the abundant $K^\pm \rightarrow \pi^\pm \pi_D^0$ and $K^\pm \rightarrow \pi^\pm \pi^+ \pi^-$ decays in order to validate the simulation.

The rate of $K^\pm \rightarrow \pi^\pm e^+ e^-$ decays is measured relatively to the rate of the abundant channel $K^\pm \rightarrow \pi^\pm \pi_D^0$ where $\pi_D^0 \rightarrow e^+ e^- \gamma$. The final states of both channels contain identical sets of charged particles. Thus electron and pion identification efficiencies, potentially representing a significant source of systematic uncertainties, do cancel at the first order.

The reconstructed $\pi^\pm e^+ e^-$ invariant mass spectrum is presented in Fig. 1. The mass resolution is $\sigma = 4.2 \text{ MeV}/c^2$, in agreement with the resolution from MonteCarlo simulation of $\sigma_{MC} = 2.3 \text{ MeV}/c^2$. A total of 7146 decay candidates are found in the signal region. After the kinematical suppression of the π_D^0 decays, residual background contamination mostly comes from particle misidentification. The following relevant background sources are identified using MonteCarlo simulations: (1) $K^\pm \rightarrow \pi^\pm \pi_D^0$ with misidentified electron and pion; (2) $K^\pm \rightarrow \pi_D^0 e^\pm \nu$ with a misidentified electron from the pion decay.

The remaining background is estimated by se-

lecting the strongly suppressed lepton number violating $K^+ \rightarrow \pi^- e^+ e^+ + \text{c.c.}$ (same-sign) events. For the above two background sources, the expected mean number of events and kinematic distributions of the selected same-sign candidates are identical to those of background events, up to a negligible acceptance correction. In total 44 events pass the same-sign selection, which leads to a background estimation of $(0.6 \pm 0.1)\%$. This result was independently confirmed using MonteCarlo simulation of the two background modes.

A total of 12.228×10^6 $K^\pm \rightarrow \pi^\pm \pi_D^0$ candidates are found in the signal region. The only significant background source comes from the semileptonic $K^\pm \rightarrow \pi_D^0 \mu \nu$ decays. Its contribution is not suppressed by particle identification cuts, since no π/μ separation is performed. The background contamination is estimated to be 0.15% by MonteCarlo simulation.

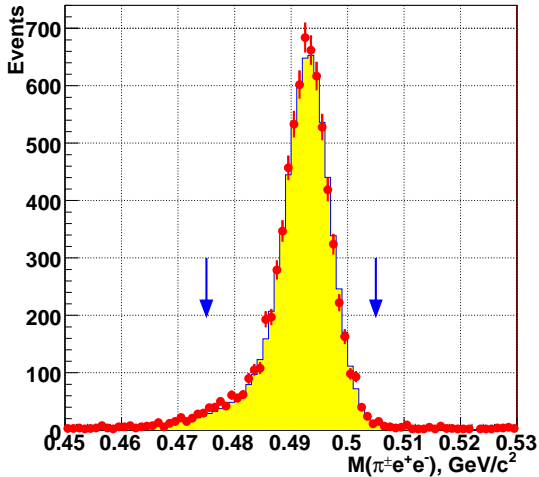


Figure 1. Distribution of reconstructed $\pi^\pm e^+ e^-$ invariant mass, data (dots) and MonteCarlo (filled area).

2.2. Fitting procedure

The value $(d\Gamma_{\pi ee}/dz)_i$ is computed in the centre of each i -bin of z as

$$\begin{aligned} (d\Gamma_{\pi ee}/dz)_i &= \frac{N_i - N_i^B}{N_{2\pi}} \times \frac{A_{2\pi}(1 - \epsilon_{2\pi})}{A_i(1 - \epsilon_i)} \\ &\times BR(K^\pm \rightarrow \pi^\pm \pi^0) \\ &\times BR(\pi_D^0) \times \Gamma_K / \Delta_z \end{aligned} \quad (2)$$

Here N_i and N_i^B are the numbers of observed $K^\pm \rightarrow \pi^\pm e^+ e^-$ candidates and background events in the i -th bin, $N_{2\pi}$ is the number of $K^\pm \rightarrow \pi^\pm \pi_D^0$ events (background subtracted), A_i and ϵ_i are geometrical acceptance and trigger efficiency in the i -th bin for the signal sample (computed by MC simulation), Γ_K is the nominal kaon width[14], and Δz is the chosen width of the z bin. The values $A_{2\pi} = 2.94\%$, $\epsilon_{2\pi} = 1.17\%$, $BR(K^\pm \rightarrow \pi^\pm \pi^0) = (20.640.08)\%$ [15] and $BR(\pi_D^0) = (1.1980.032)\%$ [14] are used. The value $(d\Gamma_{\pi ee}/dz)_i$ is then compared to the theoretical predictions, using the formula (1).

The computed values of $\Gamma_{\pi ee}/dz$ vs z are presented in Fig. 2, along with the results of the fits to the three considered models. The branching ratio $BR(K^\pm \rightarrow \pi^\pm e^+ e^-)$ in the full kinematic range corresponding to each model are then computed using the measured parameters, their statistical uncertainties, and correlation matrices. In addition, a model-independent branching ratio BR_{mi} in the visible kinematic region $z > 0.08$ is computed by integration of $d\Gamma/dz$.

2.3. Systematic uncertainties

The following sources of systematic uncertainties were studied:

- Particle identification. Despite identical charged particle composition, the signal and normalization states can differ in their momentum distributions. Therefore imperfect MonteCarlo description of electron and pion identification inefficiencies f_e and f_π can bias the result, due to the momentum dependence of the inefficiencies. Inefficiencies were measured for the data, and shown to vary in the ranges $1.6\% < f_\pi < 1.7\%$ and $1.1\% < f_e < 1.7\%$, for particle momenta in the analysis track mo-

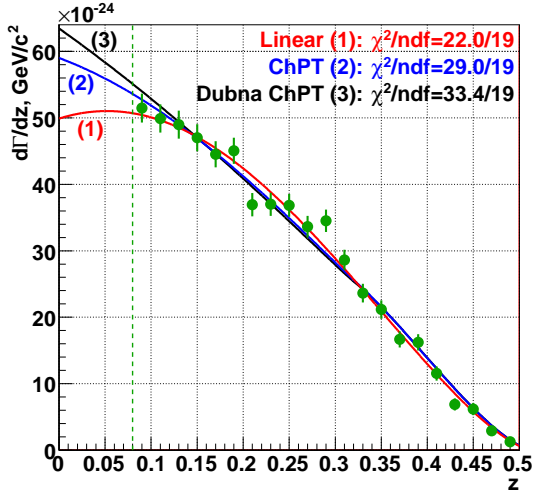


Figure 2. Distribution of $d\Gamma_{\pi ee}/dz$ for data after background subtraction and correction for trigger inefficiency. The results of the fit are shown for the three models considered.

momentum range. The associated systematic uncertainties were conservatively estimated assuming that MonteCarlo predicts momentum-independent f_e and f_π .

- **Beam line description.** A careful simulation of the beamline including time variations of its parameters was developed. Nevertheless, the residual discrepancies of data and MonteCarlo beam geometries and spectra cause a bias to the branching ratio measurements. To evaluate the related systematic uncertainties, variations of the results with respect to the cuts used for track momenta, LKr cluster energies, total and transverse momenta of the final states $\pi^\pm e^+ e^- (\gamma)$, and track distances from beam axis in spectrometer planes, were studied.
- **Background subtraction.** The same-sign event spectrum is used for background estimation in the $\pi^\pm e^+ e^-$ sample. The method has a limited statistical precision (with an

average of 2 same-sign event per bin of z). In addition, the presence of the component with two $e^+ e^-$ pairs (due to two π_D^0 decays or external conversions) biases the method, since in this case the ratio of same-sign to background is not one. The uncertainties of the measured parameters due to background subtraction were conservatively taken to be equal to the corrections themselves.

- **Trigger efficiency.** The corrections for trigger inefficiencies are evaluated by simulations. L1 and L2 corrections on decay rates have similar magnitudes of a few 10^{-3} . No uncertainty was ascribed to the L1 correction, due to relative simplicity of the trigger condition. The uncertainty of the L2 efficiency correction was conservatively taken to be equal to the correction itself.
- **Radiative corrections.** Uncertainties due to the radiative corrections were evaluated by variation of the lower $\pi^\pm e^+ e^-$ invariant mass cut.
- **Fitting method.** Uncertainties due to the fitting procedure were evaluated by variation of the z bin width.
- **External input.** Substantial uncertainties arise from the external inputs, as the $BR(\pi^\pm \pi_D^0)$ is experimentally known only with 2.7% relative precision. The only parameter not affected by the external uncertainty is the linear form factor slope δ , describing the shape of the spectrum.

The applied corrections and the systematic uncertainties (excluding the external ones which are summarized later) are shown in Table 1.

2.4. Results and discussion

The measured parameters for the various models considered, and the corresponding BRs in the full z range, as well the model-independent $BR_{mi}(z > 0.08)$, are presented in Table 2 with their statistical, systematic, and external uncertainties. The correlation coefficients between the

Table 1

Summary of corrections and experimental systematic uncertainty.

Parameter	e, π ID	Beam spectra	Background subtraction	Trigger efficiency	Rad. corr.	Fitting method
δ	0.01	0.04	-0.04 ± 0.04	-0.03 ± 0.03	0.05	0.03
f_0	0.001	0.006	0.002 ± 0.002	0.000 ± 0.001	0.006	0.003
a_+	0.001	0.005	-0.001 ± 0.001	-0.001 ± 0.002	0.005	0.004
b_+	0.009	0.015	0.017 ± 0.017	0.016 ± 0.015	0.015	0.010
M_a/GeV	0.004	0.009	0.008 ± 0.008	0.006 ± 0.006	0.009	0.006
M_b/GeV	0.002	0.003	0.003 ± 0.003	0.003 ± 0.003	0.004	0.002
$BR_{1,2,3} \times 10^{-7}$	0.02	0.02	-0.01 ± 0.01	-0.02 ± 0.01	0.01	0.02
$BR_{mi} \times 10^{-7}$	0.02	0.01	-0.01 ± 0.01	-0.02 ± 0.01	0.01	n/a

pairs of model parameters, not listed in the table, are $\rho(\delta, f_0) = -0.963$, $\rho(a_+, b_+) = -0.913$, and $\rho(M_a, M_b) = 0.998$. Fits are of reasonable quality for all the three models, however the linear form-factor model leads to the smallest χ^2 .

The obtained form factor slope δ is in agreement with the previous measurements based on $K^\pm \rightarrow \pi^\pm e^+ e^-$ [5,6] and $K^\pm \rightarrow \pi^\pm \mu^+ \mu^-$ [16] samples, and further confirms the contradiction of the data to meson dominance models[17]. The obtained f_0 , a_+ and b_+ are in agreement with the only previous measurement[6]. The measured parameters M_a and M_b are a few % away from the nominal masses of the resonances[14]. Unfortunately the data sample is insufficient to conclusively distinguish between the models considered.

The branching ratio in the full kinematic range is computed as the average between the two extremes corresponding to the models (1) and (3), and includes an uncertainty due to extrapolation into the inaccessible region $z < 0.08$: $BR = (3.08 \pm 0.04_{stat} \pm 0.04_{syst} \pm 0.08_{ext} \pm 0.07_{model}) \times 10^7 = (3.08 \pm 0.12) \times 10^7$. It should be stressed that a large fraction of the uncertainty is correlated with the earlier measurements, being due to external BRs and model dependence. A comparison to the precise BNL/E865[6] measurement dismissing correlated uncertainties, but using the same external input, shows a 1.4σ difference. In conclusion, the obtained BR is in agreement with the previous measurements.

Finally, the first measurement of the direct CP violating asymmetry of K^+ and K^- decay rates in the full kinematic range was obtained

by performing measurements separately for K^+ and K^- and neglecting the correlated uncertainties: $\Delta(K_{\pi ee}^\pm) = (BR^+ - BR^-)/(BR^+ + BR^-) = (-2.1 \pm 1.5_{stat} \pm 0.3_{syst})\%$. The result is compatible with the absence of CP violation. However its precision is far from the theoretical expectation of $|\Delta(K_{\pi ee}^\pm)| \sim 10^{-5}$ [2].

3. $K^\pm \rightarrow \pi^\pm \gamma \gamma$

The $K^\pm \rightarrow \pi^\pm \gamma \gamma$ rate is measured relatively to the $K^\pm \rightarrow \pi^\pm \pi^0$ normalization channel. The signal and normalization channels have identical particle composition of the final states, and they only differ because of a different $\gamma \gamma$ invariant mass. The trigger selection requires a minimal number of energy deposition clusters in the LKr calorimeter. About 40% of the total NA48/2 data sample have been analyzed, and 1164 $K^\pm \rightarrow \pi^\pm \gamma \gamma$ decay candidates are found, with a background contamination estimated by MonteCarlo of 3.3% (shown in Fig. ??). This has to be compared with the only previous measurement involving 31 decay candidates[9]. The reconstructed spectrum of $\gamma \gamma$ invariant mass in the accessible kinematic region $M_{\gamma \gamma} > 0.2 \text{ GeV}/c^2$ is presented in Fig. 4, along with a MC expectation assuming ChPT $O(p^6)$ distribution[7] with a realistic parameter $c = 2$. ChPT predicts an enhancement of the decay rate (cusp-like behaviour) at the $\pi \pi$ mass threshold $m_{\gamma \gamma} \approx 280 \text{ MeV}/c^2$, independently of the value of the c parameter. The observed spectrum provides the first clean experimental evidence for this phenomenon.

Table 2

Results for the fit of the 3 considered models, and the model-independent branching ratio.

$\delta =$	2.35	\pm	0.15 _{stat}	\pm	0.09 _{sys}	\pm	0.00 _{ext}	$=$	2.35	\pm	0.18
$f_0 =$	0.532	\pm	0.012 _{stat}	\pm	0.008 _{sys}	\pm	0.007 _{ext}	$=$	0.532	\pm	0.016
$BR_1 \times 10^7 =$	3.02	\pm	0.04 _{stat}	\pm	0.04 _{sys}	\pm	0.08 _{ext}	$=$	3.02	\pm	0.10
$a_+ =$	-0.579	\pm	0.012 _{stat}	\pm	0.008 _{sys}	\pm	0.007 _{ext}	$=$	-0.579	\pm	0.016
$b_+ =$	-0.798	\pm	0.053 _{stat}	\pm	0.037 _{sys}	\pm	0.017 _{ext}	$=$	-0.798	\pm	0.067
$BR_2 \times 10^7 =$	3.11	\pm	0.04 _{stat}	\pm	0.04 _{sys}	\pm	0.08 _{ext}	$=$	3.11	\pm	0.10
$M_a =$	0.965	\pm	0.028 _{stat}	\pm	0.018 _{sys}	\pm	0.002 _{ext}	$=$	0.965	\pm	0.033
$M_\rho =$	0.711	\pm	0.010 _{stat}	\pm	0.007 _{sys}	\pm	0.002 _{ext}	$=$	0.711	\pm	0.013
$BR_3 \times 10^7 =$	3.15	\pm	0.04 _{stat}	\pm	0.04 _{sys}	\pm	0.08 _{ext}	$=$	3.15	\pm	0.10
$BR_{mi} \times 10^7 =$	2.26	\pm	0.03 _{stat}	\pm	0.03 _{sys}	\pm	0.06 _{ext}	$=$	2.26	\pm	0.08

As a first step of the analysis, the partial width of the decay was measured assuming the ChPT $O(p^6)$ shape with a fixed parameter $c = 2$. The following preliminary result, which is in agreement with the ChPT computation for $c = 2$, was obtained:

$$BR = (1.07 \pm 0.04_{stat.} \pm 0.08_{syst.}) \times 10^{-6}$$

A combined fit of the $m_{\gamma\gamma}$ spectrum shape and the decay rate is in progress, to measure the c parameter.

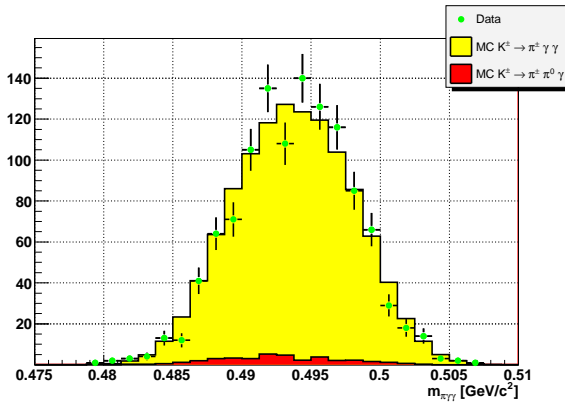


Figure 3. Distribution of $\pi^+\gamma\gamma$ invariant mass, data (dots) and MonteCarlo (filled area) calculated assuming ChPT $O(p^6)$ with $c = 2$.

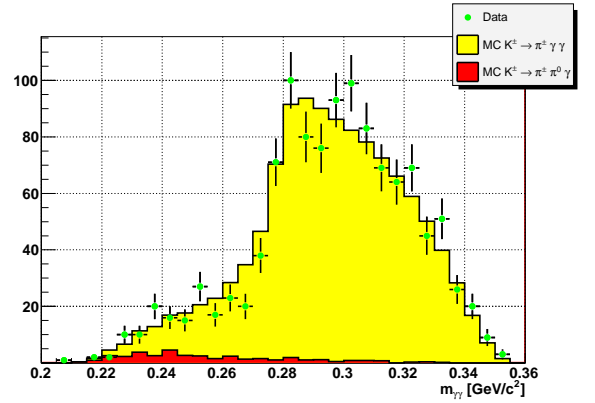


Figure 4. Distribution of $\gamma\gamma$ invariant mass, data (dots) and MonteCarlo (filled area) calculated assuming ChPT $O(p^6)$ with $c = 2$.

4. $K^\pm \rightarrow \pi^\pm \gamma e^+ e^-$

The decay $K^\pm \rightarrow \pi^\pm \gamma e^+ e^-$ has very similar kinematic to $K^\pm \rightarrow \pi^\pm \gamma\gamma$, since one of the photons here converts internally into a pair of electrons. The branching ratio can be naively estimated using the following relation:

$$BR(K^\pm \rightarrow \pi^\pm \gamma e^+ e^-) = BR(K^\pm \rightarrow \pi^\pm \gamma\gamma) \times 2\alpha = 1.6 \cdot 10^{-8}$$

where α is the fine-structure constant. The $K^\pm \rightarrow \pi^\pm \gamma e^+ e^-$ rate is measured relatively to the $K^\pm \rightarrow \pi^\pm \pi_D^0$ channel. The signal and normalization channels have identical particle composition in the final state. The same trigger selection as for $K^\pm \rightarrow \pi^\pm e^+ e^-$ decays is used. The signal is selected having an invariant mass $\pi^\pm \gamma e^+ e^-$ between 480 MeV/c² and 505 MeV/c², and requiring the invariant mass $\gamma e^+ e^-$ to be greater than 260 MeV/c².

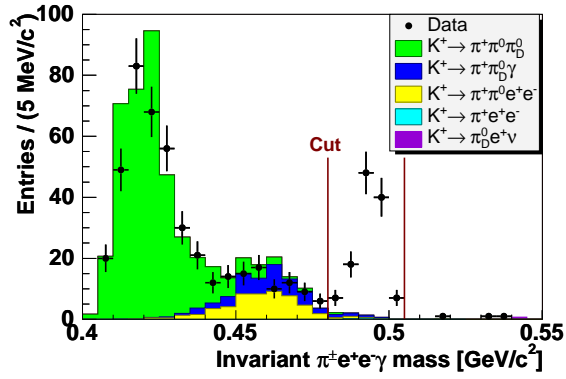


Figure 5. Distribution of $\pi^\pm \gamma e^+ e^-$ invariant mass, data (dots) and MonteCarlo expectation for background (filled area).

With the full NA48/2 data sample analyzed, 120 $K^\pm \rightarrow \pi^\pm \gamma e^+ e^-$ decay candidates are found in the accessible kinematic region $M_{\gamma ee} > 0.26$ GeV/c², with a background of 6.1%, estimated with simulation (shown in Fig. ??). The main source of background is the $K^\pm \rightarrow \pi^\pm \pi_D^0 \gamma$ with a lost photon. The distribution of the $\gamma e^+ e^-$ invariant mass is presented in Fig. 6, along with MonteCarlo predictions for the background contributions. The $\gamma e^+ e^-$ spectrum provides another evidence for the rate enhancement at the $\pi\pi$ mass threshold.

The model-independent partial width in the ac-

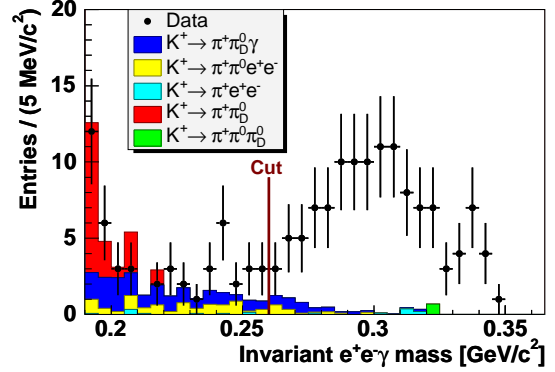


Figure 6. Distribution of $\gamma e^+ e^-$ invariant mass, data (dots) and MonteCarlo expectation for background (filled area).

cessible kinematic region is measured:

$$BR(M_{\gamma ee} > 0.26 \text{ GeV}/c^2) = (1.19 \pm 0.12_{stat.} \pm 0.04_{syst.}) \times 10^{-8}$$

The ChPT parameter c assuming $O(p^4)$ distribution[8] was measured to be $c = 0.90 \pm 0.45$. This measurement represents the first observation of the $K^\pm \rightarrow \pi^\pm \gamma e^+ e^-$ decay channel[18]

5. Conclusions

Preliminary results for the branching ratios of $K^\pm \rightarrow \pi^\pm e^+ e^-$ and decay parameters have been obtained, and they are in agreement with the previous measurements. The first limit on CP violating charge asymmetry has also been shown.

A precise study of the $K^\pm \rightarrow \pi^\pm \gamma \gamma$ has been performed. The first clear evidence for a rate enhancement at $\pi\pi$ mass threshold has been obtained. The preliminary measurement of the branching ratio agrees with the ChPT prediction. A detailed study of the spectrum shape is in progress.

The first observation of the $K^\pm \rightarrow \pi^\pm \gamma e^+ e^-$ decay, and measurement of its branching ratio and decay parameters, have been performed. The

$M_{\gamma ee}$ spectrum provides an independent evidence for a threshold effect at the $\pi\pi$ mass.

REFERENCES

1. G. Ecker, A. Pich, E. de Rafael, Nucl. Phys. B291 (1987) 692.
2. G. D'Ambrosio et al., JHEP 8 (1998) 4.
3. A.Z. Dubnickova et al., Phys. Part. Nucl. Lett. 5, vol. 2 (2008) 76 [hep-ph/0611175].
4. P. Bloch et al., Phys. Lett. B56 (1975) 201 (1975).
5. C. Alliegro et al., Phys. Rev. Lett. 68 (1992) 278 (1992).
6. R. Appel et al., Phys. Rev. Lett. 83 (1999) 4482.
7. G. D'Ambrosio, J. Portoles, Phys. Lett. B386 (1996) 403.
8. F. Gabbiani, Phys. Rev. D59 (1999) 094022.
9. P. Kitching et al., Phys. Rev. Lett. 79 (1997) 4079.
10. J.R. Batley et al., Eur. Phys. J. C52 (2007) 875.
11. GEANT detector description and simulation tool, CERN program library long writeup W5013 (1994).
12. E. Barberio and Z. Was, Comp. Phys. Comm. 79 (1994) 291.
13. R. Fruhwirth, Nucl. Inst. Methods A262 (1987) 444.
14. W.-M. Yao et al. (PDG), J. Phys. G33 (2006) 1.
15. M. Antonelli et al., arXiv:0801.1817.
16. H. Ma et al., Phys. Rev. Lett. 84 (2000) 2580.
17. P. Lichard, Phys. Rev. D60 (1999) 053007.
18. J.R. Batley et al., Phys. Lett. B659 (2008) 493.